Efficacy of Pond Ash as a Cover Material in Single and Dual Capillary Barriers

CSSU Srikanth[1*], *B J* Ramaiah[1], *A* Murali Krishna[1], and *Sai K* Vanapalli[2]

[1]Department of Civil and Environmental Engineering, IIT Tirupati, Tirupati, Andhra Pradesh, India
[2]Department of Civil Engineering, University of Ottawa, 161 Louis-Pasteur St., Ottawa, Ontario, Canada

Abstract. In this paper, numerical study results that highlight the capability of using pond ash as a cover material in covers with capillary barrier effects are succinctly summarized. A model was exclusively developed and calibrated using commercial software SEEP/W for this study. After calibration, the efficiency of pond ash as a coarse-grained layer (CGL), fine-grained layer (FGL), unsaturated drainage layer (UDL), and seepage control layer (SCL) was investigated using various combinations. The CCBE made of pond ash obtained from the output and input points of an ash pond as alternate fine- and coarse-grained layers were observed to perform well. The performance of pond ash as UDL and SCL was also observed to be good. The approach presented in this study is valuable in assessing likely slope failures of coal ash storage facilities that may be triggered by rainfall events. The study aids in significantly reducing rainfall infiltration, improving the overall stability of the slopes, and promoting sustainability by utilising the concept of "waste covering waste". The approaches used in this study can be extended in the rational design of slopes to address the future challenges anticipated with unprecedent rainfall events and its negative impacts associated with climate change effects.

1 Introduction

Covers with capillary barrier effects (CCBE) have been used as liner/cover materials to prevent rainfall infiltration into the disposal structures. They are based on the principle of capillarity where the pores in the fine-grained layer (FGL) (placed over coarse-grained soil) of the soil act as a large network of small diameter tubes (placed over the larger diameter tubes), creating suction in the bottom layer and preventing drainage from entering the coarse-grained layer (CGL). The precipitation on the surface of the fine layer is stored in the fine layer itself due to the low permeability of the soil until the water entry value of the coarse-grained soil is reached at the interface. The CCBEs perform well in the areas where the water table is low, and the water balance in the region is negative. The water stored in the fine-grained layer is sent back to the atmosphere through evaporation and evapotranspiration.

Several published research studies [1,6,7] have established the effectiveness of CCBE over other types of cover materials. Waste materials like coarse recycled aggregate (CRA) and fine recycled aggregate (FRA) [1] have been used in conjunction to propagate the idea of 'waste covering waste.' In ash ponds which are ash disposal structures constructed in the vicinity of thermal power plants, the fine pond ash and coarse pond ash are easy to locate due to the standard design procedures of ash ponds where the inlet points are abundant with coarse pond ash (CPA), and outlet points are abundant with fine pond ash (FPA) which generally consist of sand range and silt range respectively as can be seen in Fig. 1. For this reason, the key objective of the present study is to exploit the differences in the grain size distribution of FPA and CPA and evaluate their efficacy as cover materials in the CCBE.

2 Materials and Methodology

2.1 Materials utilised

In the present study, the data points of the soil water characteristic curve (SWCC) and hydraulic conductivity function (HCF) of CRA and FRA have been obtained from [1] and have been fit extending Fredlund Xing equation [2] using SEEP/W [3]. Similarly, the SWCC and HCF of pond ash from input (CPA) and output (FPA) were obtained from [5]. The SWCCs and HCFs of CRA and FRA are presented in Fig. 2, and SWCC and HCFs of CPA and FPA are presented in Fig. 3.

The breakthrough suction (su_c) in a CCBE is generally defined as the suction at which the water starts entering the coarse-grained layer, which can be interpreted as the water entry value of the coarse soil [6]. Another way of interpreting the breakthrough suction as the suction at which the HCFs of fine and coarse layers intersect [6]. It can be observed from Figs. 2b and 3b, the corresponding su_c for FRA over CRA and FPA over CPA is around 0.25 kPa and 6 kPa, respectively.

* Corresponding author: ce19d503@iittp.ac.in

https://doi.org/10.1051/e3sconf/202338221004

The capacity of the CCBE increases with decreasing su_c, as it requires almost positive or zero pressures to develop inside the coarse layer at the break-through point. This means a gravel layer that is underlain by sand layer will have a better capacity. However, for humid climatic conditions or areas with high rainfall intensity, once the breakthrough occurs, the percolation rate would be relatively high due to the ease of drainage [7].

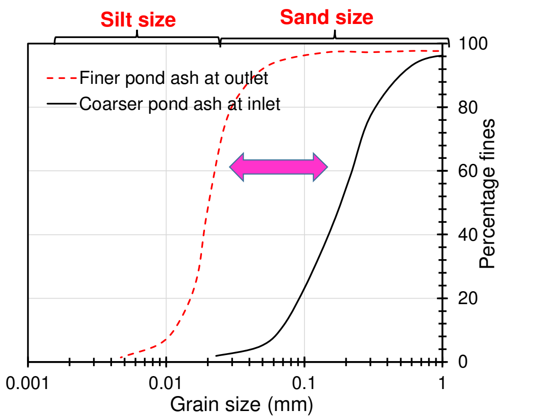

Fig. 1. Variation in grain size distribution characteristics in pond ash collected from an ash pond [4].

Hence, silt over sand layers can be utilized beneficially for extreme rainfall events as they allow limited quantity of water to percolate through them even after the breakdown [8]. This characteristic is exploited in the present study, which is discussed in the later sections.

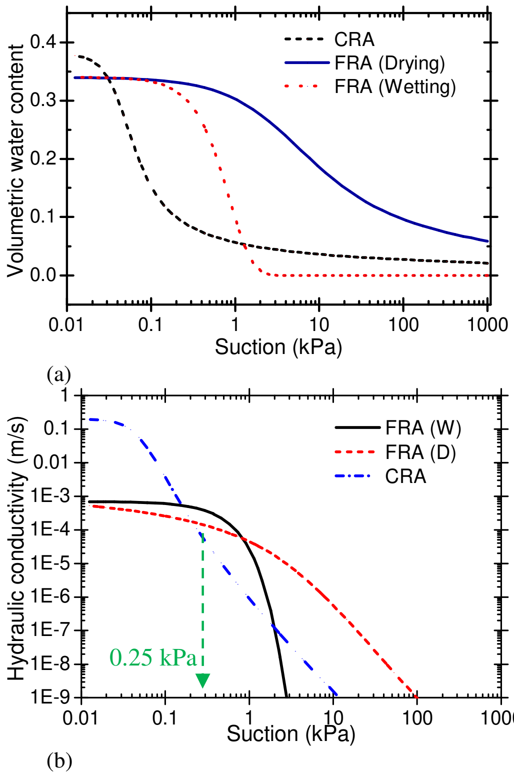

Fig. 2. (a) SWCC and (b) HCFs, of CRA and FRA considered in the study [1].

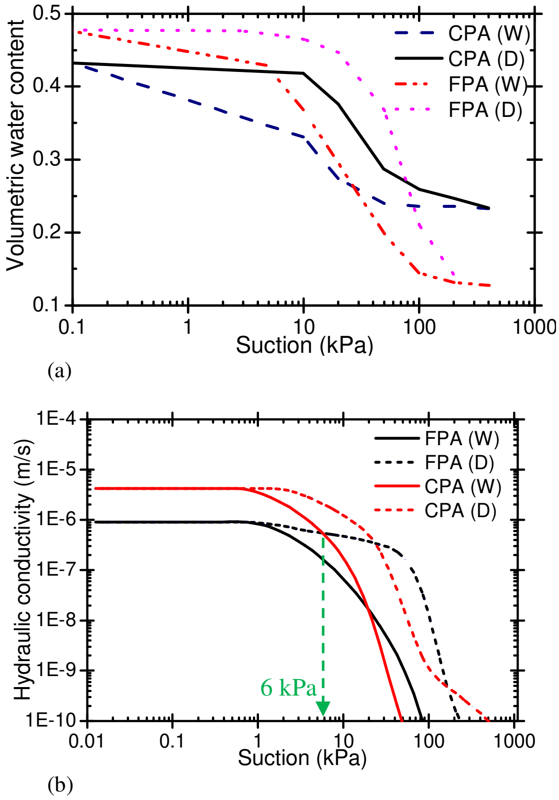

Fig. 3. (a) SWCC and (b) HCFs, of CPA and FPA considered in the study [5].

2.2 Procedure

The material properties used in the infiltration column setup in [1] were considered in the study for the purpose of calibration of the model, with CRA and FRA, as shown in Fig. 4a. The height and width of the column were taken as 1 m and 0.2 m, respectively. The volumetric water content (VWC) profiles and pore water pressure (PWP) profiles were obtained and compared with the experimental data.

Once the model was validated, the CRA and FRA were replaced, as can be seen from Fig. 4b, with CPA and FPA, and the analysis was continued. In the next combination, the CPA was placed over CRA to check if there was further improvement in the performance of CCBE. This approach is consistent with [7] where the middle sand layer acts as an unsaturated drainage layer (UDL) for the application of CCBE in humid climates. Further, the suitability of fine pond ash as a seepage control layer (SCL) was evaluated with the arrangement as shown in Fig. 4d. Finally, a dual CCBE system with FPA and CPA as alternate layers was analysed. The sequence of all the combinations is summarized in Fig. 4 for comprehensive visualisation.

3 Calibration of the model

The analysis was done in four stages: namely, upward flow, drawdown, rainfall infiltration and drainage tests.

Sub-branches were created in SEEP/W with the pore pressure profiles obtained in the previous analysis step as the initial condition in the present branch. The analysis was created as a transient analysis problem where the solution is obtained using Richard's equation. The second-order triangular elements were adopted in the numerical model with a mesh size of 0.05m. The upward flow condition was simulated by applying boundary conditions of 1.52 m head at the bottom, similar to experimental conditions. The upward-flow stage allowed the materials to gradually saturate. Once the saturated volumetric content was attained throughout the material, a subsequent draw down stage was performed. For the drawdown condition scenario, a zero water pressure head boundary condition was applied at the bottom to drain out all the water, to achieve a similar steady-state initial condition in all cases and to simulate the unsaturated conditions present in the field.

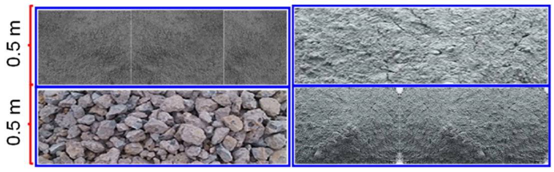

(a) FRA over CRA (b) FPA over CPA

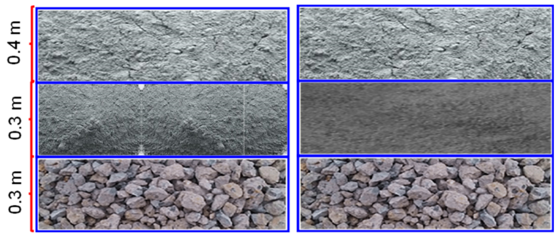

(c) FPA over CPA and CRA (d) FPA over FRA and CRA

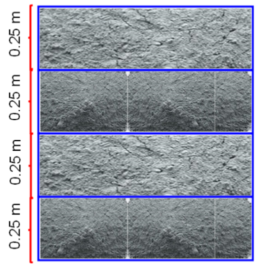

(e) Dual CCBE consisting of FPA, CPA, FPA, and CPA

Fig. 4. Visualisation of CCBEs considered in the study.

The rainfall infiltration was divided into multiple substages, each lasting for 6 hours [1]. During each substage, a specific rainfall intensity (4 mm/h, 8 mm/h, and 40 mm/h) was applied. After each substage, the sample was allowed to drain and stabilize for 24 hours prior to the beginning of next substage. A delayed rainfall pattern was chosen in all cases where the intensity gradually increases to the maximum value at the end of the rainfall duration. In all the stages, a zero-flux boundary condition was applied at the side boundary; in other words, they were considered impenetrable walls with zero net inflow /outflow. The boundary conditions applied in each of the stages are presented in Fig. 5 and they were held consistent in each stage for all combinations.

The pore pressure profiles deviated in the fine-grained material during all stages because of the complications in replicating the exact conditions in real-world scenarios as shown in Fig. 6a. However, the steady-state profiles developed after each stage closely resembled the 24-hour pore-water pressure (PWP) profile used in the experiment.

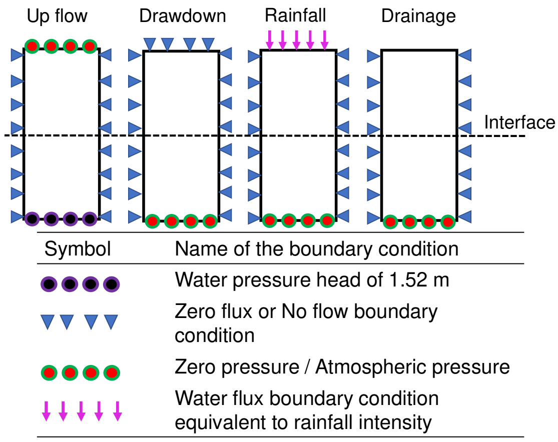

Fig. 5. Boundary conditions used in the present study.

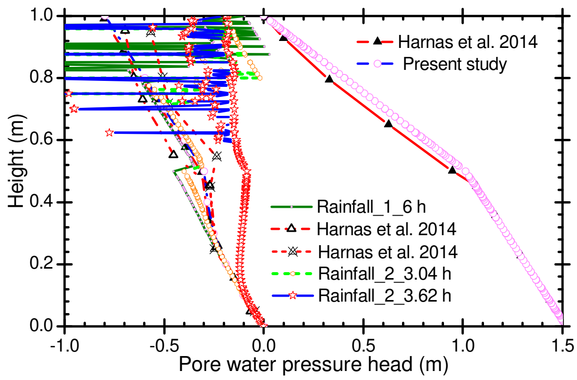

(a)

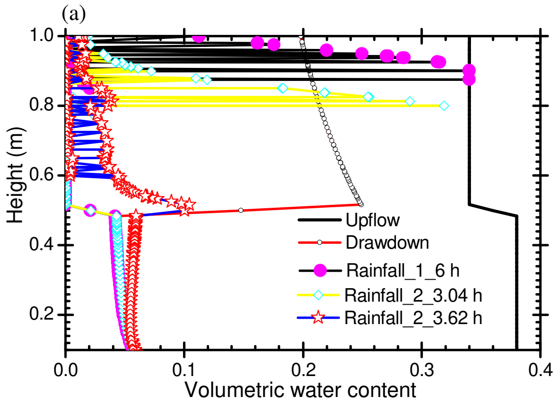

(b)

Fig. 6. (a) Pore water pressure profiles of FRA over CRA, (b) Visualisation of break-through suction through VWC profiles.

Further, the time for breakthrough suction was obtained by observing the change in PWP and VWC profiles along with the increase in domain water volume. The breakthrough occurred between 3 and 3.62

 https://doi.org/10.1051/e3sconf/202338221004

hours from the start of the second stage rainfall, as shown in Fig. 6b, where a change in VWC and PWP profiles can be observed in this period. The result matched closely with [1] (break-through suction time of 3 hours). Hence, the model was considered calibrated, and the same model was used for evaluating the efficacy of pond ash as FGL and CGL, UDL and SCL in a CCBE.

However, the water entry value of coarse pond ash is not near zero (it is around 5 – 20 kPa), which limits the maximum capacity of the CCBE in terms of breakthrough suction.

One of the major advantages is associated with the wide permeability range of fine and coarse-grained layers, which assists in the retainment of water in the barrier in an extreme rainfall event. As a result, water percolation is relatively low in this study, even after the PWP at the capillary break (which was considered as zero suction at the interface) is reached.

4 Results and Discussion

4.1 FPA over CPA

The analysis was done by maintaining all the geometrical and boundary conditions consistent with calibrated model by replacing the fine and coarse-grained layers with FPA and CPA, respectively. However, one additional stage was added (after rainfall 2) with a rainfall intensity of 40 mm/h to investigate the capability of CCBE in extreme rainfall events. In addition, the drawdown stage was extended to 10 days to allow the equilibration of PWPs. Wetting SWCC was used for upward-flow and rainfall stage while drying SWCC was used for the drawdown and drainage stage to account for the hysteresis and simulate real field conditions. The PWP and VWC profiles obtained for the present combination are plotted in Fig. 7.

A major shift in PWP and VWC can be observed at 12.5 days (i.e., 6 hours after the advent of Rainfall 2 (8 mm/h)). Hence, the performance of FPA over CPA can be considered satisfactory compared to FRA over CRA. There can be two reasons for the increment in functioning capability. First, the hydraulic conductivity coefficient of FPA over the CPA system is relatively low, which allows the system to retain water for longer times. In addition, for the same thickness, the CPA is already at break-through condition compared to CRA (0.5 m for CPA and 0.02 m for CRA). Due to this reason, the functioning of CPA over the FPA can be considered conservative.

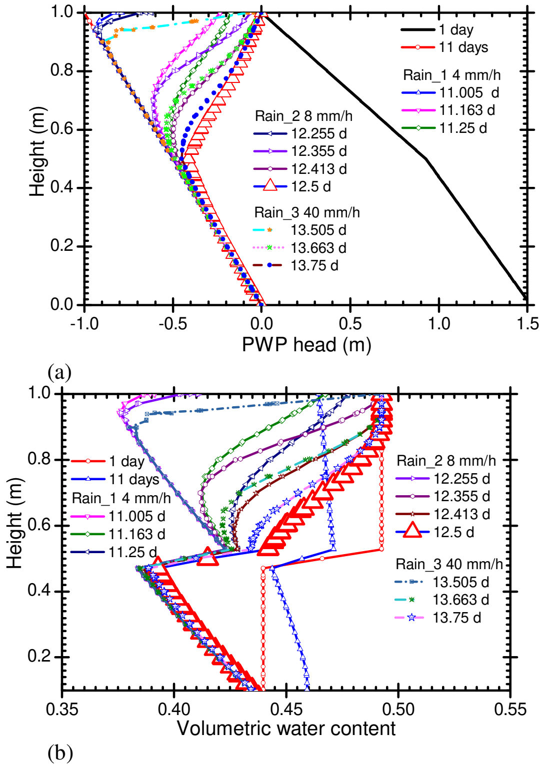

Fig. 7. (a) PWP and (b) VWC profiles for FPA over CPA.

4.2 FPA over CPA and CRA

In the existing combination, the efficacy of pond ash as a UDL was evaluated. As discussed earlier, using gravel size as a coarse layer is disadvantageous because of the high percolation of water once the break occurs. Hence, the main function of the UDL is to act as a smooth transition between the finer silt range material and coarser gravel range material and allow steady drainage once the capillary break occurs. The influence of sandwiched CPA layer can be visibly understood from the PWP and VWC profiles plotted in Fig. 8.

Even if the capillary break at the first interface occurs 6 hours after the occurrence of Rainfall 2 condition (i.e., 8 mm/h), which is similar to the previous combination, the break-through at the second interface only happens 6 hours after the advent of Rainfall 3 (i.e., 40 mm/h) due to the presence of an additional layer. Hence, FPA over CPA and CRA system has withstood the extreme rainfall event for a longer duration. Moreover, adding a gravel layer at the bottom can be much more beneficial for the attainment of an all-weather-resistant CCBE system. The present combination also helps in a smooth transition in the grain size distribution from silt to gravel, which further helps the cause of stability by avoiding intermixing of particles.

 https://doi.org/10.1051/e3sconf/202338221004

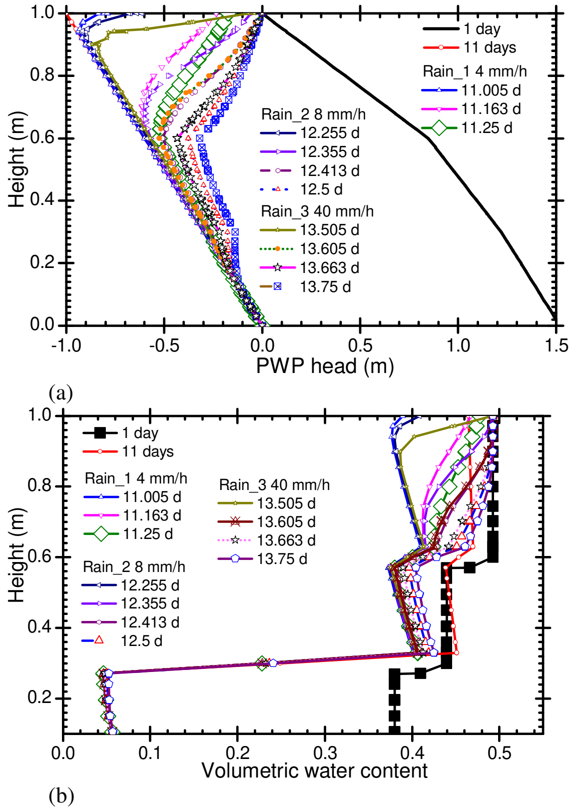

Fig. 8. (a) PWP and (b) VWC profiles for FPA over CPA and CRA.

4.3 FPA over FRA and CRA

The main limitation of the FRA and CRA layer was the sudden increase in the amount of water intake post-failure. Hence, the functioning of pond ash as SCL was tested in the present combination by placing FPA over FRA and CRA. The results are presented in Fig. 9. The first break occurs at the end of Rainfall 2 (8 mm/h) which is similar to the previous scenario. The system was resilient to VWC and PWP changes even after the end of Rainfall 3 (40 mm/h). Such a behavior may be attributed to the top layer that acts as a percolation control layer, and as a result, the capillary action is maintained in the bottom layers.

4.4 Dual CCBE with alternating layers of FPA and CPA

In the final combination, the effect of dual capillarity on the CCBE was investigated. For this purpose, FPA and CPA were altered to create three interfaces and were subjected to the same conditions applied previously. The results are presented in Fig. 10. The dual CCBE responded reasonably to all three rainfall stages. The capillary break happened 6 hours after the start of Rainfall 3, where a change in PWP and VWC was observed in the second interface, while the third interface was near the capillary break.

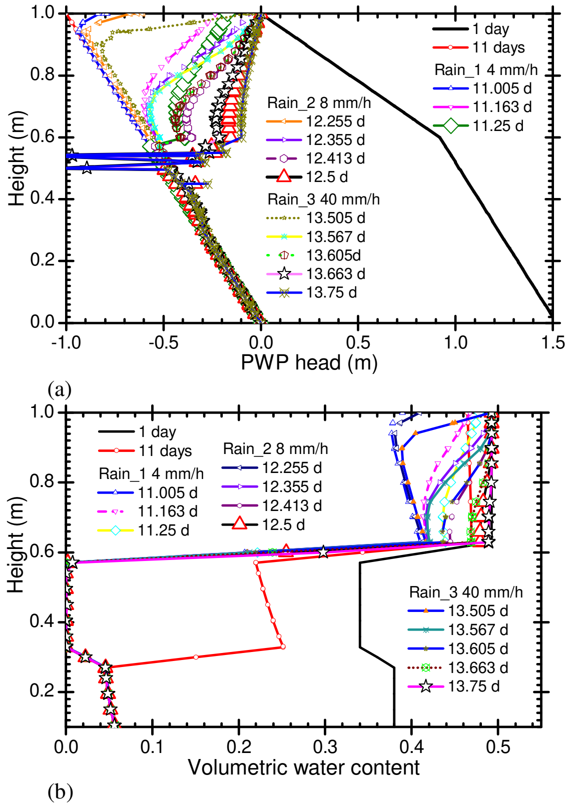

Fig. 9. (a) PWP and (b) VWC profiles for FPA over FRA and CRA.

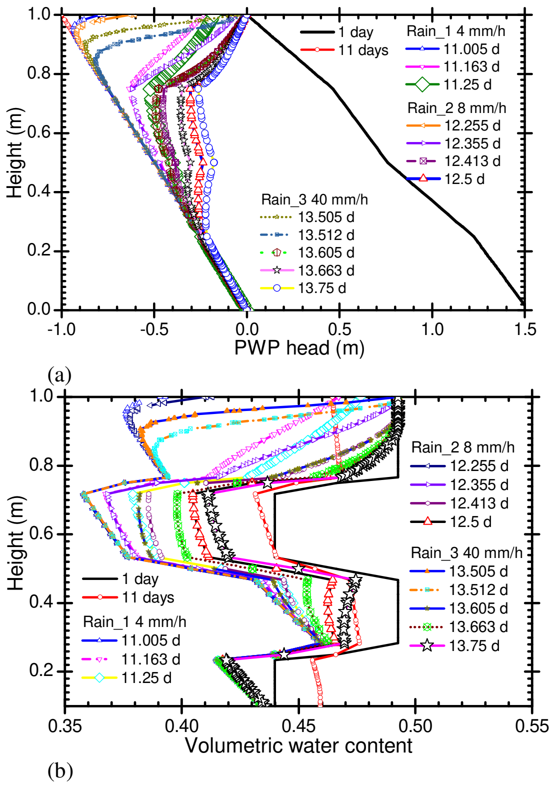

Fig. 10. (a) PWP and (b) VWC profiles for dual CCBE (FPA over CPA, FPA, and CPA).

4.5 Variation of PWP and domain water volume with time

The change of PWP at interfaces and domain water volume was evaluated with respect to time by further continuing the study; the obtained results are summarized and plotted in Figs. 11 and 12. The FRA over CRA had the highest PWP head change in the Rainfall 2 period, while the dual CCBE system had the highest PWP head in the Rainfall 3 period. The three-layer CCBEs had an overall better performance in terms of reducing percolation and the PWPs. However, the dual CCBE system was effective in reducing water infiltration.

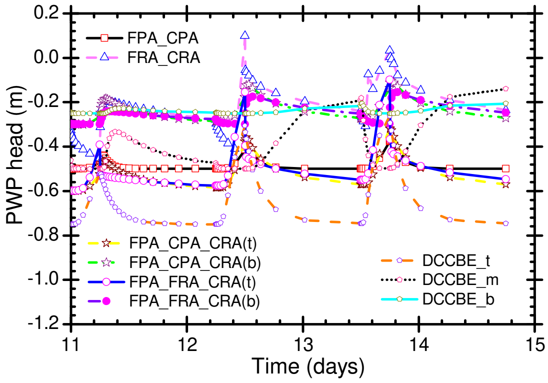

Fig. 11. Variation of PWP head across interfaces with time.

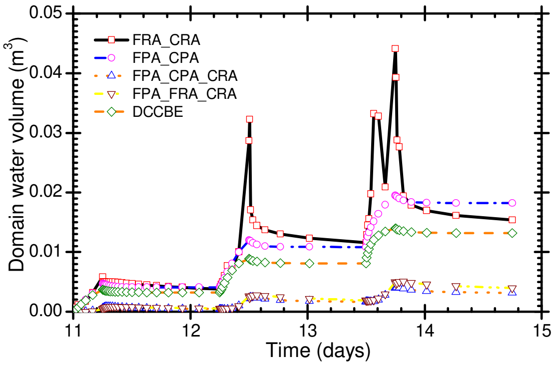

Fig. 12. Variation of domain water volume with time.

5 Conclusions

In the current study, numerical analysis has been performed to investigate the efficiency of pond ash as cover material in CCBE. The model was evaluated for different combinations of pond ash as FGL, CGL, UDL, and SCL, and the results were presented in terms of VWC and PWP profiles. The conclusions of the study are as follows:

➢ The sand over gravel (FRA over CRA) CCBEs tend to perform well till breakthrough but allow sudden inflow of water after their failure, which is one of the major causes of concern. In contrast, silt over sand (FPA over CPA) tends to retain more water due to its less permeability. However, they are prone to capillary break due to higher water entry value and a right shift in the intersection of HCF curves of FGL and CGL.

➢ The three-layer CCBE performed well in terms of PWP and VWC profiles. In addition, overall percolation and change in PWP on failure were also on the lower side. Hence, either of the two 3-layer CCBEs can be considered an all-weather CCBE.

➢ The performance of CPA as UDL was observed to be satisfactory. In spite, of the first break that can likely happen at a similar time, the presence of the middle layer would help in extending the time for failure of the entire system.

➢ FPA as an SCL can contribute to an increase in the resistance of the single-layered CCBE tremendously. The FPA over FRA and CRA is the best combination that will not break even after the application of heavy rainfall during the third stage.

➢ The dual CCBE performed better in the first two stages of rainfall; however, once the failure happened in the third stage, it recorded the highest PWP head change at the interface compared with all the systems. The variations in grain size distribution that manifest during the disposal of coal ash in an ash storage facility; however, can be further exploited for their use as cover materials in inclined CCBEs.

Acknowledgments

Authors would like to express their gratitude to Ms. Mengxi Tan, a doctoral scholar at the Department of Civil Engineering, University of Ottawa, for her insightful comments on the numerical modelling aspects of this study.

References

1. F.R. Harnas, H. Rahardjo, E.C. Leong, J.Y. Wang, Canadian Geotechnical Journal. **51**, 10 (2014).
2. D. G. Fredlund, A. Xing. Canadian Geotechnical Journal. **31**, 521-532 (1994).
3. Geo-Slope International Ltd. Seep/W user's manual for seepage modeling. (Calgary, Alta: GEO-SLOPE International Ltd, 2012).
4. R.S. Jakka, G.V. Ramana, M. Datta, Geotechnical and Geological Engineering. **28**, 763–778 (2010).
5. J. Singh, S.K. Singh, Indian Geotechnical Journal. **49**, 341-351 (2019).
6. J.H. Li, L. Du, R. Chen, L.M. Zhang, Computers and Geotechnics. **48**, 304-315 (2013).
7. T.L.T. Zhan, H. Li, G.W. Jia, Y.M. Chen, D.G. Fredlund, Canadian Geotechnical Journal. **51**, 12, 1438-1448 (2014).
8. D. Tami, H. Rahardjo, E.C. Leong, D.G. Fredlund, Canadian Geotechnical Journal. **41**, 814-830 (2004).